IEEE Access
Multidisciplinary | Rapid Review | Open Access Journal

Received April 20, 2020, accepted May 4, 2020, date of publication May 11, 2020, date of current version May 22, 2020.

*Digital Object Identifier 10.1109/ACCESS.2020.2993628*

# Optimal Control of AVR System With Tree Seed Algorithm-Based PID Controller

**ERCAN KÖSE**
Electrical-Electronics Engineering Department, Tarsus University, 33400 Tarsus, Turkey
e-mail: ekose@tarsus.edu.tr

**ABSTRACT** In this study, an optimal Tree-Seed Algorithm (TSA) algorithm-based Proportional-Integral-Derivative (PID) controller is proposed for automatic voltage regulator (AVR) system terminal tracking problem. PID controller gains $K$p, $K$i, and $K$d are optimized with the proposed TSA algorithm based on different objective functions. The TSA-based optimal PID controller's performance is compared with numerous PID controllers, which were developed using different meta-hermetic optimization algorithms in the literature. Several analysis methods including root locus, bode analysis, robustness, and disturbance rejection are studied and compared with reported works in the literature. It is shown that there is still a research gap to improve the tracking performance of the AVR system due to its importance in electrical systems. According to the obtained comparison results, it has been revealed that the proposed TSA-based PID controller improves tracking properties under load change thus it can be effectively used for synchronous generator automatic voltage regulator terminal voltage stability.

**INDEX TERMS** Automatic voltage regulator, tree-seed algorithm, PID controller, transient response, root locus, bode analysis, robustness, disturbance analysis.

## I. INTRODUCTION

The electrical loads change the behavior of the generators and the output load supply voltages. Keeping the value of the output voltage of the generator against dynamic load change is essential and it has been an important engineering problem. Many studies have been reported in this subject recently [1]–[6]. Some of these studies are based on an automatic voltage regulator (AVR) to control the generator output voltage. For the AVR system to function properly, a controller is required because of the generator output voltage drop is inevitable in such systems.

Generator output voltage drop can lead to increased line losses, higher current draws to achieve the desired power, fluctuations in voltage, power cuts, unstable states on transmission lines, and damage to the loads. Damage to the systems as a result of these events causes financial issues in the design viewpoint. It is then essential to report existing solutions to better analyze the problem. Wang *et al.* present a systematic approach to evaluate the technical and potential economic impacts resulting from voltage drop disorders from customers' perspective [7]. Martinez and Martin-Arnedo use a medium-sized distribution network for the stochastic estimation of voltage drops based on the Monte Carlo method after providing a summary of studies on voltage drop analysis using a time-effect domain [8]. Wang *et al.* state that the voltage drop could lead to economic losses that cause hundreds of thousands of dollars, and they created an error tree analysis to represent the relationship between device sensitivity to voltage drops and transactions with high economic consequences in case of interruptions. They demonstrate that the need to concentrate on more financially useful measures by taking into account system performance, device tolerances, and the impact of device failures on the manufacturing process and associated economic losses [9]. In another study [10], Chen *et al.* demonstrate the effects of voltage drops on electrical users, as well as the losses of electrical users' suffering from voltage drops. They conduct a cost-benefit analysis to prevent voltage drop. They also demonstrate that it can cause major loss for industrial users using stable electricity.

The nominal output voltage of the generator should be kept constant to prevent high financial cost due to voltage drop. AVR tries to keep the output voltage at nominal level by changing the generator excitation voltage against changing loads. The researchers to achieve this goal have applied a number of control techniques to formulate a good closed-loop structure of the AVR system. Some of these studies are as follows. Gaing optimally calculated the coefficients

The associate editor coordinating the review of this manuscript and approving it for publication was Mohsin Jamil.

of a PID controller with PSO algorithm, and examine the results in detail [11]. Chatterjee and Mukherjee investigate the applicability of the teaching-learning based optimization algorithm to the computation of PID coefficients of an AVR system containing a first-order low-pass filter [12]. Ekinci and Hekimo lu propose an improved Kidney-Inspired algorithm (IKA) as a new approach to optimally calculate the coefficients of a PID controller in the AVR system. Their quantitative analysis provides an important inference for literature studies. They also demonstrate a comparative transient state analysis with numerical simulation results [13]. Rahimian and Raahemifar use an PSO algorithm to design a high order AVR system's optimum PID controller parameters. They define a new cost function. Thanks to this cost function for providing stable convergence feature, fewer number of iterations, and fast tuning of optimum PID controller parameters [14]. As a different approach, Anbarasi and Muralidharan develop a bacterial foraging optimization algorithm-based PID controller using a new objective function design to improve the performance of the AVR system. They compare their approach with other meta-heuristic algorithm results in the literature [15]. Bahgaat and Hassan explore several adaptive PSO methods for the AVR system of a synchronous generator to achieve the best tuned parameters of the PID controller, which increase the stability margin and improves the performance of the system [16]. Ortiz-Quisbert *et al.* propose a fractional order model reference adaptive control and fractional order PID control for the AVR system. PSO and GA optimization algorithms are used to calculate the optimal coefficients of the proposed control systems. The results of the proposed controllers in terms of advantages and disadvantages are compared with the case study based on the literature results [17]. Modabbernia *et al.* present an $H_\infty$ controller as a new approach for the AVR system to demonstrate a solid operating performance. $H_\infty$ controller is proposed and compared to PID and fuzzy logic-based PID results are compared [18]. Gil-González *et al.* give the dynamic model of a synchronous machine for hydro-turbine governing systems with automatic voltage regulator. They develop a passivity-based controller to regulate the voltage in multi-machine power systems that guarantee the stability properties [19]. Ribeiro *et al.* propose an SM-PI controller based on sliding-mode control and PI control hybridization to adjust the output terminal voltage of a synchronous generator connected to the power grid. They show that the proposed SM-PI controller effectively suppresses voltage oscillations, preventing instability in the system [20]. Aribowo introduce a Focused Time Delay Neural Network controller method for the AVR system. It uses the load angle and speed criteria to test the performance of the improved controller [21]. Batmani and Golpîra follow a systematic approach, which is based on an optimal quadratic tracking design for the AVR system. They use an adaptive dynamic programming (ADP) method to solve this optimal control problem [22]. Salman *et al.* developed artificial intelligence techniques for AVR and Load-Frequency-Control for an PID controller design [23]. Rakshit and Maity design an AVR system that can convert in dual conversion depending on the use of Sim Power system components in MATLAB/Simulink environment [24]. This converter consists of PI controlled three phase inverter and fuzzy logic controlled Cuk converter system.

Although the control techniques mentioned above have been employed in the AVR system successfully, PID (Proportional-Integral-Derivative) controller is generally preferred. The reason behind this is that the PID controller is relatively cheap and easy in real-time. In order for the PID controller to be effective in the AVR, the coefficients of the controller should be optimally determined. To this end, it is necessary to look into the literature. Gözde and Toplamacioglu calculated the optimal coefficients of the parameters of the PID controller with ABC (artificial bee colony), PSO (particle swarm optimization), and DE (differential evolution) algorithms. They compare transient responses, root locus, bode diagrams, and statistical receiver operating characteristic (ROC) analysis results, showing the performance of the system based on their optimal coefficients. They show that the performance of the ABC algorithm is better in terms of the transient analysis of the output voltage [25]. To determine the coefficients of the PID controller based on Lozi Map, a chaotic optimization method is utilized by Coelho. Numerical results show that their proposed algorithm presents a good behavior in AVR system [26]. Razmjoy *et al.* have developed a new meta-heuristic optimization algorithm inspired by the FIFA World Cup Competitions (WCO) for the PID controller, employed to the AVR system. They also use genetic algorithm (GA) and PSO algorithm to compare the performance of their method. According to their analysis, it is revealed that WCO algorithm is preferred [27]. Bingul and Karahan use the CS (Cuckoo Search) algorithm for the novel tuning of the PID controller in the AVR design. They compare the output voltage performance in terms of maximum overshoot, rise time, settling time, and steady-state error performance criterias. Also, PSO and ABC algorithms are studied to compare the performance of the proposed CS algorithm. In addition to these comparisons, they achieve a good robustness performance under disturbances and parametric uncertainties [28].

In this study, we use a tree-seed algorithm (TSA)-based PID controller for the AVR system. The proposed algorithm optimally calculates the values of PID coefficients. TSA is a robust and powerful metaheuristic algorithm based on swarm intelligence. The convergence speed performance of the algorithm is also better than its peers in the literature [29]. Therefore, it has been widely preferred in engineering design problems and numerical optimization calculations in recent years. The main underlying idea behind the TSA is based on the natural phenomena of trees and their seeds [29]. The TSA algorithm is implemented for many studies in the literature. Gungor *et al.* utilize an TSA algorithm for high dimensional continuous optimization problems. Experimental study shows that the TSA represents better robustness and convergence characteristics [30]. Uney and Cetinkaya employ an TSA algorithm for reactive power losses [6].

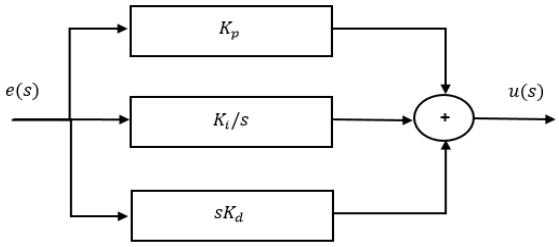


**FIGURE 1.** PID controller schematic structure.

In [31], an TSA algorithm is proposed to state of charge estimation in the Li-Ion Batteries [31].

In this study, TSA algorithm is proposed to optimally calculate the coefficients of PID controller in the AVR system. Then, IKA, local unimodal sampling (LUS), ABC, PSO, DEA, pattern search algorithm (PSA) and biogeography based optimization (BBO) algorithms and literature results are compared to show the performance of the proposed tree-seed algorithm. The comparison results revealed that the TSA-based PID controller algorithm improves voltage reference tracking in the AVR system.

Contributions are formally stated as follows:

1) Tree seed algorithm is used to AVR voltage regulation first time

2) The proposed method is quantitatively compared with existing works to highlight achieved improvements by taking into account various assessment criteria

3) The compatibility/flexibility of proposed approach under various scenarios are tested with conventional objective functions.

4) Many analysis methods are used including root locus, bode analysis, disturbance rejection, and robustness to ensure the real-time workings of the proposed algorithm in an AVR system.

The structure of this paper is as follows. Section II briefly introduces the concept of PID controller, Section III defines a generic AVR model with its main components for control design, Section IV defines objective function and tree seed algorithm is demonstrated in Section V. Section VI represents a comprehensive analysis results of finding, and lastly Section VII concludes the paper.

## II. PID CONTROLLER

PID controllers are the most widely used controllers in industrial applications. This is due to its simple structure and presenting good performance behavior. PID controller schematic structure is shown in Figure 1. Here, $K_{\mathrm{p}}$ is the proportional, $K_{\mathrm{i}}$ is the integral and $K_{\mathrm{d}}$ is the derivative gain coefficients. The transfer function of a PID controller is given (1) [32].

$$G_{PID}(s) = \frac{u(s)}{e(s)} = K_p + \frac{K_i}{s} + K_d s \tag{1}$$

## III. AVR SYSTEM MODELING

An AVR system is modeled with four first-degree subsystem structure. These subsystems are expressed as amplifier, exciter, generator, and sensor in the literature [13], [26], [27]. The closed-loop AVR model structure is given in Figure 2.

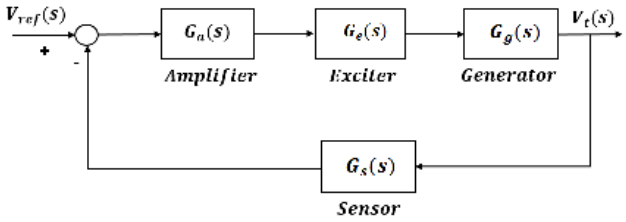


**FIGURE 2.** Closed loop AVR model structure.

**TABLE 1.** AVR system constants.

| Ranges of the gain and time | Selected gains and time constants |
|---|---|
| $10 \le K_a \le 40$ | $K_a = 10$ |
| $1.0 \le K_e \le 10$ | $K_e = 1.0$ |
| $0.7 \le K_g \le 1.0$ | $K_g = 1.0$ |
| $K_s = 1.0$ | $K_s = 1.0$ |
| $0.02 \le T_a \le 0.1$ | $T_a = 0.1$ |
| $0.5 \le T_e \le 1.0$ | $T_e = 0.4$ |
| $1.0 \le T_g \le 2.0$ | $T_g = 1.0$ |
| $0.001 \le T_s \le 0.06$ | $T_s = 0.01$ |

Commonly used gains and time constants are seen in Table 1.

To compare the results of this study with the results of the literature, the constants of the transfer functions $G_a(s)$ , $G_e(s)$, $G_g(s)$ and $G_s(s)$ [11], [13], [32]–[35] are taken as the references. In Table 1, the ranges and selected values of these constants are given in detail. Moreover, system components are

The amplifier model is given by

$$G_a(s) = \frac{K_a}{1 + \mathrm{s}T_a} = \frac{10}{1 + 0.1\mathrm{s}} \tag{2}$$

The exciter transfer function is given by a gain and a time constant as

$$G_e(s) = \frac{K_e}{1 + \mathrm{s}T_e} = \frac{1}{1 + 0.4\mathrm{s}} \tag{3}$$

The generator is represented by a transfer function as,

$$G_g(s) = \frac{K_g}{1 + \mathrm{s}T_g} = \frac{1}{1 + 1\mathrm{s}} \tag{4}$$

The first-order transfer function of sensor model is

$$G_s(s) = \frac{K_s}{1 + sT_s} = \frac{1}{1 + 0.01s} \tag{5}$$

Using (2), (3), (4) and (5), we calculate the closed-loop transfer function of the AVR system, leading to (6)

$$G_{AVR}(s) = \frac{V_t(s)}{V_{ref}(s)} = \frac{G_a(s)\,G_e(s)\,G_g(s)}{1 + G_s(s)\,G_a(s)\,G_e(s)\,G_g(s)} = \frac{0.1s + 10}{0.0004s^4 + 0.045s^3 + 0.555s^2 + 1.51s + 11} \tag{6}$$

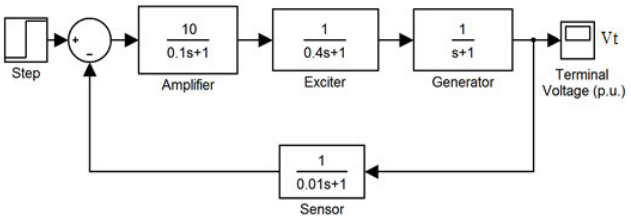


**FIGURE 3.** The without control AVR system Simulink model for unit step response.

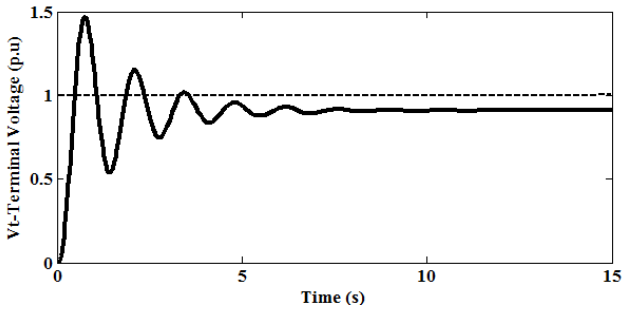


**FIGURE 4.** Terminal output voltage change of the without controller AVR systems.

**TABLE 2.** AVR system response.

| Criteria | Response values |
|---|---|
| $M_p$% | 65.4272% (Peak value =1.5039 p.u.) |
| $\boldsymbol{t_s}$ | **6.9711 s (±2%)** |
| $t_r$ | 0.2607 s |
| $\boldsymbol{t_p}$ | **0.7547 s** |
| $E_{ss}$ | 0.0907 |

The AVR system without a controller is given with (6). The dynamic behavior of this system can be observed by a unit step response. For this, a Simulink model is constructed and depicted in Figure 3. In addition, the unit step response of AVR system without controller as the terminal voltage change is given in Figure 4. Here, terminal voltage is shown as per-unit (p.u.) base unit quantity system. It is the expression of system quantities per unit as fractions of a defined basic unit quantity. The power, voltage, current, impedance, and admittance values used in electricity can be given as per-unit.

As observed from Figure 4, the output voltage is not tracking the desired reference thus a controller is needed to eliminate the steady-state error as well as reducing the settling time. The AVR system open-loop system characteristics $M_p$, $t_s$, $t_r$, and $E_{ss}$ are given in Table 2. The AVR system poles and zero are demonstrated in Table 3. In addition, the stability behavior of the system can be seen by examining the poles of the transfer function of the AVR system. The zero-poles of the AVR system are given in Table 3. The system has a pair of conjugate poles. These conjugated poles cause the damped oscillation in the system.

**TABLE 3.** AVR system zero-poles.

| Zero-Poles | Values |
|---|---|
| Two real poles | $S_1$= -98.8170+0i, $S_2$=-12.46261+0i |
| **Two complex poles** | **$S_3$= -0.5285-4.6649i, $S_4$= -0.5285-4.6649i** |
| One Zero | Z= -100+0i |

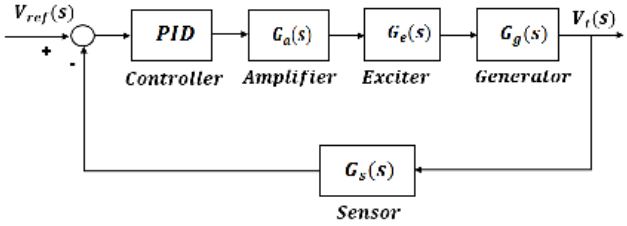


**FIGURE 5.** The closed loop-AVR model structure with PID.

Generator output voltage, transient state behavior should be improved and the steady-state error should be reduced to zero. In order to achieve these, that is, to bring the system to a point that will show an optimal behavior, a high performance controller must be added to the system. In this study, PID controller is chosen for the control of AVR system. Closed-loop control structure of the AVR system with PID controller is given in Figure 5. Transfer function of the closed-loop PID controlled AVR system given is presented in (7), as shown at the bottom of this page.

## IV. OBJECTIVE FUNCTIONS

In general, the method of IAE, ISE, ITSE, and ITEA are often used to evaluate PID controller design performance in the literature [11], [13], [36]–[38]. Instead of evaluating these error criterias as only objective, Zwe-Lee Gaing's study demonstrated that the aim of the combinations of these error criterias, which include weight factors, is a better way to form a common objective [11]. Many researchers use the presented method [13], [18], [28], [39].

The objective function according to Zwe-Lee Gaing approach (W (K)) is defined as follows,

$$W(K) = \text{MinF}(k_p, k_i, k_d) = \left(1 - e^{-\beta}\right)\left(M_p + E_{ss}\right) + e^{-\beta}(t_s - t_r) \quad (8)$$

$$G_{AVR}(s) = \frac{V_t(s)}{V_{ref}(s)} = \frac{G_{PID}(s) G_a(s) G_e(s) G_g(s)}{1 + G_{PID}(s) G_a(s) G_e(s) G_g(s) G_s(s)} = \frac{0.1K_d s^3 + \left(0.1K_p + 10K_d\right) s^2 + \left(0.1K_i + 10K_p\right) s + 10K_i}{0.0004s^5 + 0.0454s^4 + 0.555s^3 + \left(1.51 + 10K_d\right) s^2 + (1 + 10K_p)s + 10K_i} \quad (7)$$

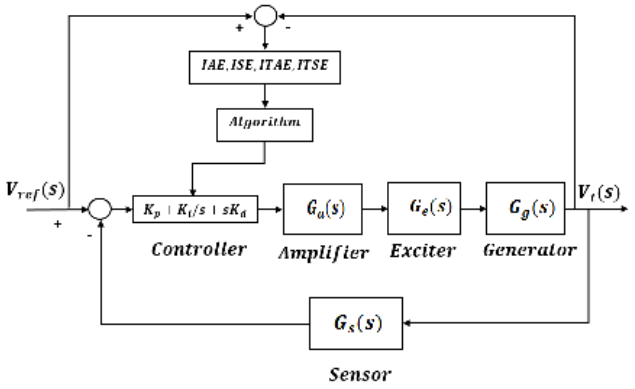


**FIGURE 6.** The closed loop-AVR model structure with PID controller using TSA algorithm.

The $\beta$ is the weighting factor. The core objective is to eliminate the tracking error as follows.

$$ITAE = \int_0^t t\,|V_r - V_t|dt = \int_0^t t\,|e|dt \tag{9}$$

$$IAE = \int_0^t |V_r - V_t|\,dt = \int_0^t |e|\,dt \tag{10}$$

$$ITSE = \int_0^t t\,|V_r - V_t|^2 dt = \int_0^t t\,|e|^2 dt \tag{11}$$

$$ISE = \int_0^t |V_r - V_t|^2\,dt = \int_0^t |e|^2\,dt \tag{12}$$

Numerous objective functions have been described in the literature to determine that the PID controller optimally improves the dynamic behavior of the system. Objective functions are including $M_p$, $t_r$, $t_s$, and $E_{ss}$ control design criteria. It is the performance indicator for the AVR system to have minimum values of these criteria for a unit step response. The other objective functions [39],

$$OF_1 = \propto_1 x\ ITAE + \propto_2 xT_s + \propto_3 M_p \tag{13}$$

$$OF_2 = \propto_1 x\ IAE + \propto_2 xT_s + \propto_3 M_p \tag{14}$$

$$OF_3 = \propto_1 x\ ITSE + \propto_2 xT_s + \propto_3 M_p \tag{15}$$

$$OF_4 = \propto_1 x\ ISE + \propto_2 xT_s + \propto_3 M_p \tag{16}$$

In the analysis, we first quantitatively compare the above objective functions to better choose the right method in this sequel.

In this study, TSA algorithm have been proposed for tuning the parameters of the PID controller. The proposed algorithm obtains the PID controller coefficients optimally based on the objectives defined above. The closed loop-AVR model structure with PID controller using TSA algorithm have been shown in Figure 6.

## V. PROPOSED ALGORITHM

### A. TREE-SEED ALGORITHM (TSA)

TSA is a population-based, nature-inspired, and stochastic as well as one of the commonly used metaheuristic optimization algorithms. TSA that is based on the relation among to trees

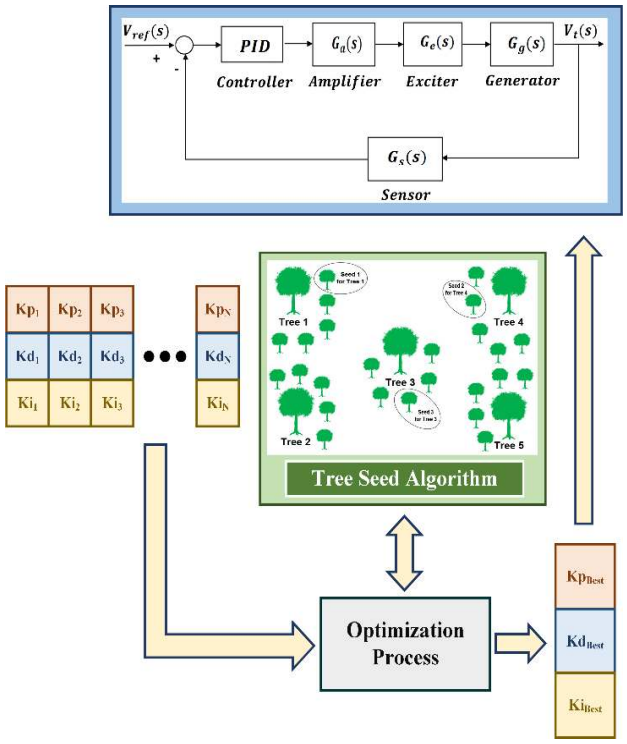


**FIGURE 7.** The TSA basic flow diagram for AVR system optimization.

and seeds is developed by Kiran [29] to solve the continuous optimization problems. The reproduction and propagation mechanism of trees population are performed by the seeds. The transportation of seeds is changed in accordance with its structures and shapes. Some of seeds hold on to the feathers of birds, furs of animals, and clothes. They are moved from the tree to different places. In this way, the seeds grow in the proper environment and they become the trees. In TSA, the ground is taken into consideration as the search space for optimization problems. Both seeds and trees are represented the solutions of optimization problems. The exploitation and exploration processes are very significant for the high performance of the meta-heuristic algorithms and achieving a more efficient solution. In the exploration phase, the tree into search space are randomly dispersed and then the seeds having characteristically similar with the trees are utilized in the phase of exploitation. The following expressions are used to produce the seeds.

$$S_{k,j} = T_{i,j} + \alpha_{i,j} x (B_j - T_{r,j}) \tag{17}$$

$$S_{k,j} = T_{i,j} + \alpha_{i,j} x (T_{i,j} - T_{r,j}) \tag{18}$$

where, $S_{k,j}$ is $j^{th}$ dimensional parameter of the $k^{th}$ seed produced from $i^{th}$ tree, $T_{i,j}$ is the $j^{th}$ dimensional parameter of $i^{th}$ tree, $B_j$ is $j^{th}$ dimensional parameter for the best location of tree obtained so far, $T_{r,j}$ is $j^{th}$ dimensional parameter of the $r^{th}$ tree that is chosen randomly in tree society, $\alpha_{i,j}$ is the scaling factor randomly produced in [−1,1]. The best seed is determined by perform a greedy selection among to the seeds of each tree in the process of search. The TSA is proceeded

**TABLE 4.** Parameters PID for different objective functions.

| Algorithm/ Parameters | OF1 | OF2 | OF3 | OF4 |
|---|---|---|---|---|
| TSA/Kp | 0.9649 | 1.1641 | 1.0625 | 0.9656 |
| TSA/Ki | 0.6710 | 0.8260 | 0.9977 | 1.5323 |
| TSA/Kd | 0.3110 | 0.4661 | 0.2853 | 0.8035 |

**TABLE 5.** Parameters TSA-PID for different objective functions.

| Functions | Over shoot | Peak Overshoot | Peak Time | Settling Time | Rise Time |
|---|---|---|---|---|---|
| OF1 | **10.3578** | **1.1036** | 0.4239 | 0.9259 | 0.2005 |
| OF2 | 14.5920 | 1.1459 | 0.3191 | 0.8201 | 0.1491 |
| OF3 | 13.8237 | 1.1382 | 0.2982 | **0.7686** | 0.1393 |
| OF4 | 19.9983 | 1.2 | **0.2340** | 2.8243 | **0.1055** |

**TABLE 6.** PID parameters for different algorithms.

| Algorithms using ITSE | Kp | Ki | Kd |
|---|---|---|---|
| TSA (proposed) | 1.1281 | 0.9567 | 0.5671 |
| IKA [13] | 1.0426 | 1.0093 | 0.5999 |
| LUS [39] | 1.2012 | 0.9096 | 0.4593 |
| ABC [33] | 1.6524 | 0.4083 | 0.3654 |
| PSO [34] | 1.7774 | 0.3827 | 0.3184 |
| DEA [33] | 1.9499 | 0.4430 | 0.3427 |
| PSA [42] | 1.2771 | 0.8471 | 0.4775 |
| BBO [43] | 1.2464 | 0.5893 | 0.4562 |

**TABLE 7.** Transient response for different algorithms.

| Algorithms using ITSE | Overshoot | Peak Over shoot | Peak Time | Settling Time | Rise Time |
|---|---|---|---|---|---|
| TSA (proposed) | 15.57 | 1.155 | 0.278 | 0.758 | 0.131 |
| IKA [13] | 15.00 | 1.150 | 0.269 | 0.753 | 0.128 |
| LUS [39] | 15.46 | 1.154 | 0.313 | 0.799 | 0.151 |
| ABC [33] | 24.85 | 1.248 | 0.375 | 3.093 | 0.157 |
| PSO [34] | 29.92 | 1.299 | 0.374 | 3.399 | 0.163 |
| DEA [33] | 32.74 | 1.327 | 0.359 | 2.650 | 0.154 |
| PSA [42] | 16.84 | 1.169 | 0.316 | 0.804 | 0.144 |
| BBO [43] | 15.52 | 1.155 | 0.317 | 1.446 | 0.149 |

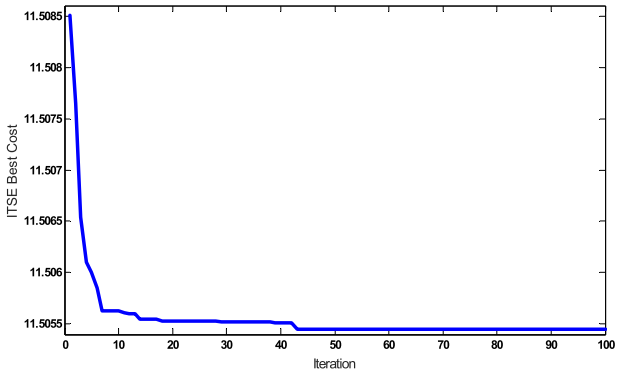


**FIGURE 8.** The convergence curves for ITSE objective functions using TSA algorithm.

as far as the termination criteria. The TSA basic flow diagram showing this situation is shown in Figure 7.

The objective function values obtained according to (13-16), whose PID coefficients are optimized with the TSA algorithm, are given in Tables 4 and 5. OF1, OF2, OF3, OF4 are objective functions including ITAE, IAE, ITSE, ISE respectively. When the transient performance objectives of OF1, OF2, OF3 and OF4 in Table 5 are examined, it can be observed that OF1 represents the best result in terms of overshoot, OF3 gives the minimum settling time, OF4 gives the minimum peak time and rise time. According to these transient response results, ITSE can be used in analysis. Since settling time is with ITSE objective gives the best result, we employ the ITSE objective to computation of PID controller gains in the simulation results section.

The TSA transient responses in Table 7 are obtained according to the ITSE objective function. With these results, it is appropriate to compare the OF3 function transient response because both functions present mutual objectives. Our results show that ITSE exhibits better performance in terms of transient response quantities.

## VI. SIMULATION RESULTS

IKA, LUS, ABC, PSO, DEA, PSA, and BBO optimization algorithms are widely used in the literature and we analyse the performance of the proposed TSA algorithm by comparing to them. In the literature, the algorithms mentioned above have been used for calculating PID control system parameters based on the ITSE objective function criteria. To this end, we use the ITSE objective in optimization of PID parameters with TSA algorithm proposed in this study. The $K$p, $K$i, and $K$d parameters of the PID controller, which are optimized by TSA, IKA, LUS, ABC, PSO, DEA, PSA, and BBO optimization algorithms are given in Table 6, and the unit step terminal voltage transient response obtained using these PID parameters are demonstrated in Table 7. In addition, unit step terminal voltage changes with different PID designs are shown in Figures 9 and 10.

### A. CONVERGENCE PERFORMANCE

The TSA basic flow diagram showing this situation is given in Figure 7, and the convergence curve is shown in Figure 8.

In the optimization process, performed by the TSA, the population size, iteration number, and search tendency are 50, 100 and 0.1, respectively. In addition, simulations have been carried out with Matlab software and with a computer hardware Intel (R) Core (TM) i7 3.4 GHz processor and 8 GB RAM memory.

As comparing with the other heuristic or evolutionary algorithms, the TSA needs less parameter and it has much simple, easy to implement. TSA's powerful search ability performs the optimization process in a short time [29], [40]. Because, TSA is fulfilled the search process by using two different equations, it causes the creating multiple solution. This situation provides the balanced local and global search

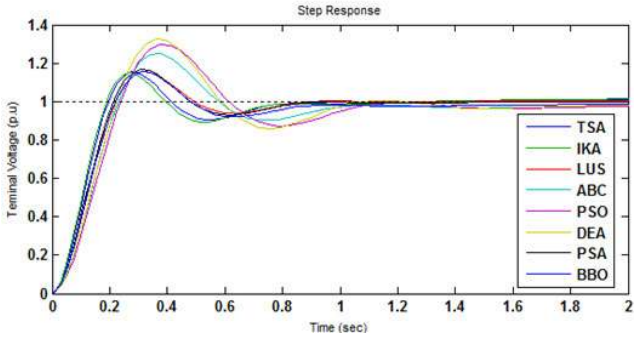


**FIGURE 9.** AVR system terminal voltage curves for TSA algorithm.

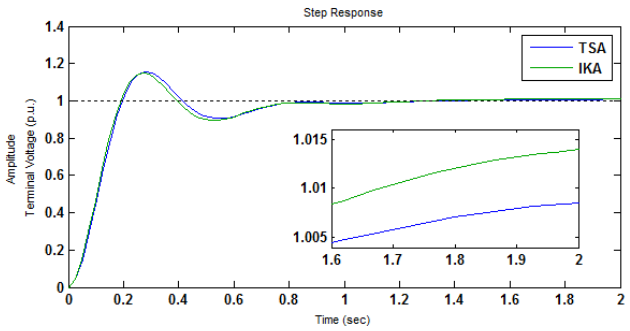


**FIGURE 10.** AVR system terminal voltage curves for TSA and IKA algorithms.

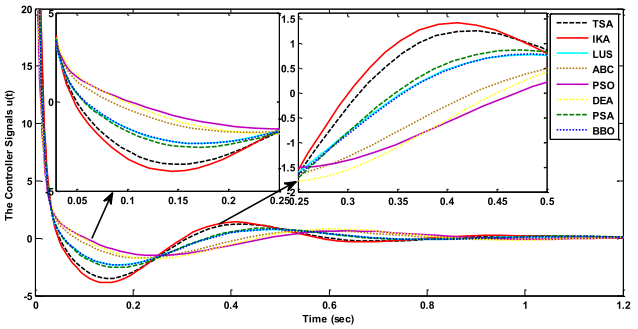


**FIGURE 11.** The optimal controller signals for the AVR system.

ability for the algorithm. Moreover, TSA can find the optimal possible solutions or points compared to other points in the search space, thanks to its search ability.

In TSA, as the search tendency parameter grows, the exploitation and convergence ability of the algorithm increases. In the opposite case, its converge is slow and the exploration ability is provided for the algorithm. Search and convergence ability of TSA can be controlled by the tendency parameter [41].

### B. TRANSIENT RESPONSE

The system's overshoot, peak overshoot, peak time, settling time, and rise time values based on the proposed TSA and reference IKA [13] algorithms are very close to each other, as

**TABLE 8.** Poles and damping ratios of AVR system.

| Controller | Close loop poles | Damping ratio |
|---|---|---|
| | **-101.55** | **1.00** |
| | **-5.05 + 11.32i** | **0.74** |
| | **-5.05 - 11.32i** | **0.74** |
| **TSA-PID** | **-0.93 + 0.82i** | **0.40** |
| | **-0.93 - 0.82i** | **0.40** |
| | -102 | 1.00 |
| | -5.13+11.7i | 0.40 |
| *IKA-PID* | -5.13-11.7i | 0.40 |
| | -0.80+0.93i | 0.65 |
| | -0.80-0.93i | 0.65 |
| | **-101.25** | **1.00** |
| | **-1.24 + 0.56i** | **0.91** |
| | **-1.24 - 0.56i** | **0.91** |
| ***LUS-PID*** | **-4.88 + 9.88i** | **0.44** |
| | **-4.88 - 9.88i** | **0.44** |
| | -100.98 | 1.00 |
| | -3.76 + 8.41i | 0.40 |
| | -3.76- 8.41i | 0.40 |
| *ABC-PID* | -4.75 | 1.00 |
| | -0.25 | 1.00 |
| | **-100.85** | **1.00** |
| | **-3.09 + 7.80i** | **0.36** |
| ***PSO-PID*** | **-3.09 - 7.80i** | **0.36** |
| | **-6.26** | **1.00** |
| | **-0.22** | **1.00** |
| | -100.91 | 1.00 |
| | -3.03 + 8.19i | 0.34 |
| *DEA-PID* | -3.03 - 8.19i | 0.34 |
| | -6.30 | 1.00 |
| | -0.23 | 1.00 |
| | **-101** | **1.00** |
| | **-1.28+0.15i** | **0.99** |
| *PSA-PID* | **-1.28-0.15i** | **0.99** |
| | **-4.82+10.1i** | **0.43** |
| | **-4.82-10.1i** | **0.43** |
| | -100 | 1.00 |
| | -4.80+10.2i | 0.427 |
| *BBO-PID* | -4.80-10.2i | 0.427 |
| | -2.1 | 1.0 |
| | -0.585 | 1.0 |

observed in Table 6. To demonstrate the achieved improvement by the proposed algorithm, Figure 11 is given. In Figure 11, it is clearly seen that the IKA algorithm's steady-state error value is higher than that of the TSA algorithm.

According to the transient response analysis results given in Table 7 ; the peak time for TSA algorithm is 12.58% less than of the LUS algorithm, 34.89% less than of the ABC algorithm, 34.53% less than of the PSO algorithm 29.13% less than of the DEA algorithm, 13.66% less than of the PSA algorithm, and 14.02% less than of the BBO algorithm. The settling time for TSA algorithm is 5.4% less than of the LUS algorithm, 308.02% less than of the ABC algorithm, 348.43% less than of the PSO algorithm, 249,6% less than of the DEA algorithm, 6.06% less than of the PSA algorithm, and 90.76% less than of the BBO algorithm. The rise time for TSA algorithm is 15.26% less than of the LUS algorithm, 19.84% less than of the ABC algorithm, 24.42% less than of

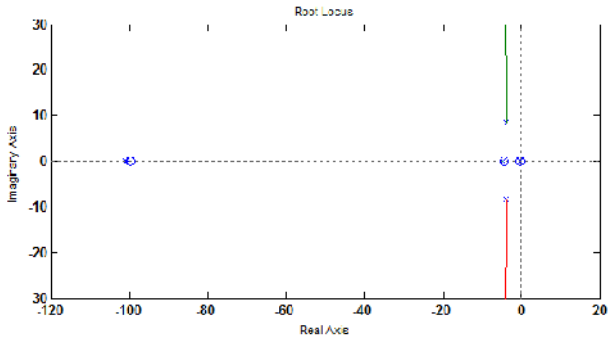


**FIGURE 12.** Root locus change graph of AVR system based on ABC.

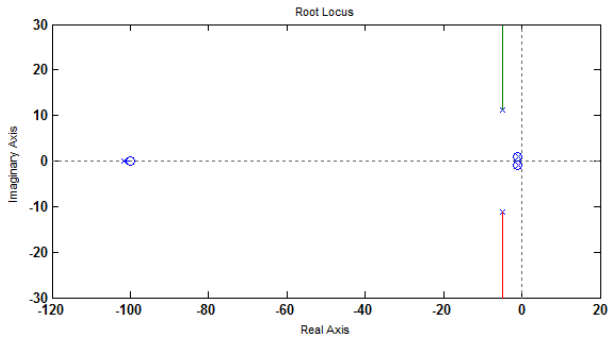


**FIGURE 13.** Root locus change graph of AVR system based on TSA.

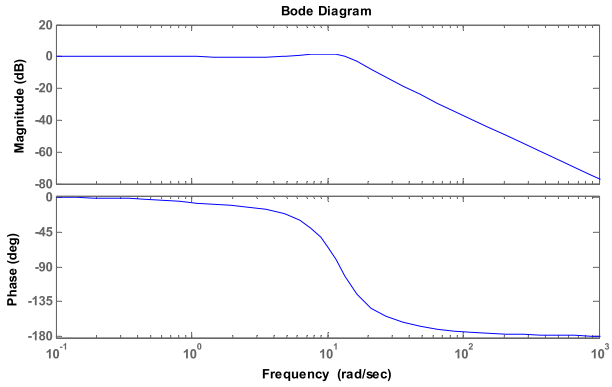


**FIGURE 14.** Bode magnitude and phase change analysis of AVR system based on TSA algorithm.

the PSO algorithm, 17.55% less than of the DEA algorithm, 9.92% less than of the PSA algorithm, and 13.74% less than of the BBO algorithm.

The control signal is an important factor in any control system design. The controller signals obtained based on the reported optimization results for the AVR system are shown in Figure 9.

### C. ROOT LOCUS

The Root Locus analysis for the AVR system tuned by TSA, IKA, LUS, ABC, PSO, DEA, PSA, and BBO are shown. The damping ratio of the poles have been calculated based on root locus, and reported in Table 8. In addition, TSA and ABC

**TABLE 9.** The results of bode analysis.

| Different algorithm | Peak Gain (dB) | Phase Margin (degree) | Delay Margin (sec) | Bandwidth |
|---|---|---|---|---|
| TSA (pro.) | 1.70(1.51Hz) | 77.39 | 0.0999 | 16.232 |
| IKA [13] | 1.78 (1.68 Hz) | 76.70 | 0.095 | 16.785 |
| LUS [39] | 1.42(1.36 Hz) | 83.24 | 0.1257 | 14.208 |
| ABC [33] | 2.84 (1.2 Hz) | 69.39 | 0.1109 | 12.879 |
| PSO [34] | 3.75(1.14 Hz) | 62.18 | 0.1033 | 12.182 |
| DEA [33] | 4.19(1.21Hz) | 58.36 | 0.0916 | 12.800 |
| PSA [42] | 1.68 ( Hz ) | 79.70 | 1.115 | 14.636 |
| BBO [43] | 1.56 ( Hz ) | 81.60 | 0.122 | 14.284 |

**TABLE 10.** AVR system robustness analysis fore based on tsa algorithm.

| Parameter | Rate of change (%) | $M_p$ (p.u.) | $t_s$ (sec) | $t_s$ (sec) | $t_p$ (sec) |
|---|---|---|---|---|---|
| *nominal* | **0** | **1.1557** | **0.7580** | **0.1332** | **0.2788** |
| $T_a$ | -50 | 1.0468 | 0.9260 | 0.1559 | 0.2293 |
| | -25 | 1.1112 | 0.7834 | 0.1224 | 0.2417 |
| | +25 | 1.1883 | 0.8098 | 0.1437 | 0.3118 |
| | +50 | 1.2135 | 0.8649 | 0.1534 | 0.3418 |
| $T_e$ | **-50** | 1.2127 | 1.1663 | 0.0868 | 0.1960 |
| | **-25** | 1.1809 | 1.0464 | 0.1109 | 0.2404 |
| | **+25** | 1.1357 | 0.8126 | 0.1543 | 0.3135 |
| | **+50** | 1.1228 | 0.8318 | 0.1755 | 0.3769 |
| $T_g$ | -50 | 1.3008 | 1.2606 | 0.0815 | 0.1818 |
| | -25 | 1.2156 | 1.0671 | 0.1080 | 0.2430 |
| | +25 | 1.1093 | 0.8160 | 0.1589 | 0.3381 |
| | +50 | 1.0763 | 2.3915 | 0.2067 | 0.3596 |
| $T_s$ | **-50** | 1.1278 | 0.7777 | 0.1370 | 0.2771 |
| | **-25** | 1.1415 | 0.7676 | 0.1350 | 0.2778 |
| | **+25** | 1.1703 | 0.7512 | 0.1315 | 0.2801 |
| | **+50** | 1.1852 | 0.7446 | 0.1299 | 0.2817 |

response curves are shown Figure 12 and 13. All poles of the PID based AVR Closed Loop system set by all algorithms are to the left of the s-plane. Therefore, AVR systems are stable.

### D. CLOSED-LOOP POLES AND BODE ANALYSIS

Bode analysis is a useful method for analyzing the frequency response of a control system. Frequency behavior of AVR system based on TSA algorithm is obtained using bode analysis method. The magnitude and phase graphical changes obtained are given in Figure 14. Comparative bode analysis results based on TSA, IKA, LUS, ABC, PSO, DEA, PSA, and BBO are shown in Table 9. In Table 9, results based on peak gain, phase margin, delay margin and bandwidth are given. Bode analysis results for TSA algorithm given in Table 9. We can see that closed-loop poles are located are in the left half plane of s-plane thus presenting a good frequency response behavior. It has minimum peak gain, maximum phase margin, minimum delay margin and maximum bandwidth values.

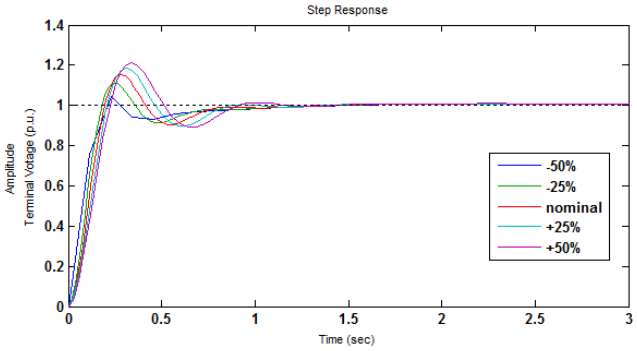


**FIGURE 15.** Terminal voltage responses for $T_a$ varying from −50% to +50%.

**TABLE 11.** Transient disturbance response for different algorithms.

| Algorithms | IAE | ISE | ITSE | ITAE |
|---|---|---|---|---|
| TSA (proposed) | 0.2127 | 0.1047 | 0.0121 | 0.1156 |
| IKA [13] | 0.2184 | 0.1028 | 0.0125 | 0.1331 |
| LUS [39] | 0.2138 | 0.1126 | 0.1272 | 0.1032 |
| ABC [33] | 0.3097 | 0.1329 | 0.0214 | 0.2261 |
| PSO [34] | 0.3417 | 0.1465 | 0.0237 | 0.2492 |
| DEA [33] | 0.3404 | 0.1461 | 0.0278 | 0.2422 |
| PSA [42] | 0.2139 | 0.1118 | 0.0127 | 0.1183 |
| BBO [43] | 0.2432 | 0.1138 | 0.0135 | 0.1486 |

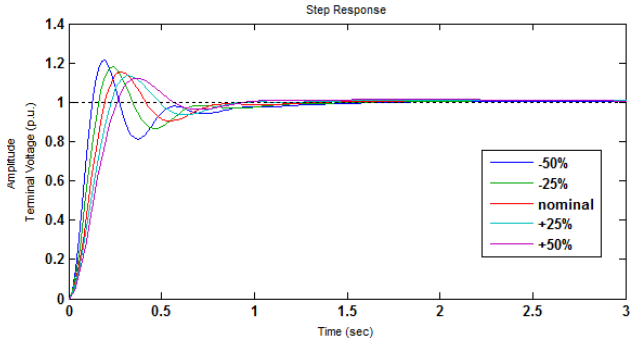


**FIGURE 16.** Terminal voltage responses for $T_e$ varying from −50% to +50%.

TSA algorithm results revealed that it provides better frequency response results than other algorithms.

### E. ROBUSTNESS ANALYSIS

In order to analyze the robustness of the PID controller based on the proposed TSA algorithm, the generator gain and time constants are changed in the range of −50% to +50% in steps of 25% and results are examined in this sequel.

Transient response analysis results obtained in line with these change intervals are shown in Table 10. It is revealed that the TSA-based PID controller exhibits more robust behavior against uncertainties in AVR parameters.

### F. DISTURBANCE AND AVR SYSTEM BEHAVIORS ANALYSIS

Load changes in synchronous generators can be modeled via disturbances. Robustness and transient response behaviors of controllers against these disturbances is important. This

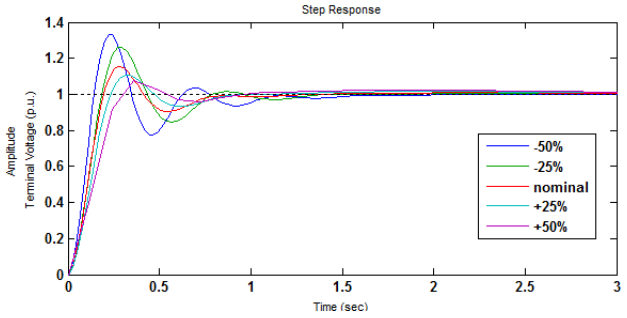


**FIGURE 17.** Terminal voltage responses $T_g$ varying from −50% to +50%.

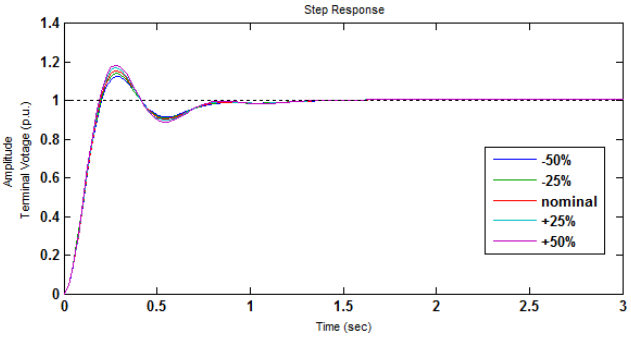


**FIGURE 18.** Terminal voltage responses for $T_s$ varying from −50% to +50%.

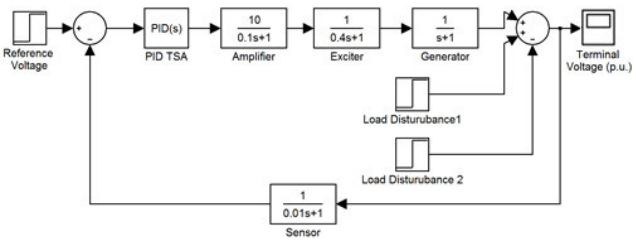


**FIGURE 19.** Simulink disturbance model for AVR system.

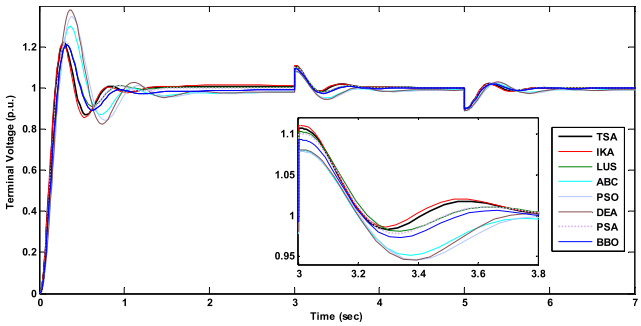


**FIGURE 20.** The AVR system disturbance responses for based on different algorithms.

structure is given in Figure 19 in MATLAB /Simulink environment. The disturbance signals in accordance with reference [28] are applied to the system at the rate of ± 10% at 3 and 5 seconds. The responses of the AVR system based on TSA-based PID controller reported and compared to the

literature in Figure 20. Also based on this, system IAE, ISE, ITSE and ITEA error criteria results are obtained at 3.5 seconds (critically evaluated) are given in Table 11.

According to the obtained IAE, ISE, ITSE and ITAE error criteria answers, TSA algorithm exhibits an improved performance.

## VII. CONCLUSION

In this study, the TSA-based PID control algorithm is proposed for optimal control of AVR. TSA algorithm is based on relation among trees and seeds. TSA is run in finding of the optimal values of the PID controller coefficients that are $K$a, $K$i and $K$p. The achieved results illustrate that the proposed AVR system with TSA optimized PID controller exhibits better performance in terms of transient and steady state responses of its voltage tracking performance as compared with the existing algorithms reported for the AVR in the literature. IKA, LUS, ABC, PSO, DEA, PSA, and BBO in the literature are quantitatively compared with TSA algorithm. These analytical results are given in Table 4 - 11 and Figures 10-18 and 20. From transient response analysis, the system's overshoot, peak overshoot, peak time, settling time and rise time values based on the proposed TSA algorithm are reported. It is revealed that even though IKA algorithm's transient responses analysis results are a bit better than TSA, TSA algorithm presents much better performance against steady state errors and disturbance. The obtained results can be interpreted that the TSA optimized PID controller proposed for the AVR system is robust against uncertainties in system parameters, meaning that the PID controller based on the proposed TSA algorithm performs better than the PID controller based on the aforementioned algorithms in the literature for synchronous generator AVR systems.

## REFERENCES

[1] X. Meng, P. Zhang, Y. Xu, and H. Xie, "Construction of decision tree based on C4.5 algorithm for online voltage stability assessment," *Int. J. Electr. Power Energy Syst.*, vol. 118, Jun. 2020, Art. no. 105793.
[2] M. Xie, M. M. Gulzar, H. Tehreem, M. Y. Javed, and S. T. H. Rizvi, "Automatic voltage regulation of grid connected photovoltaic system using Lyapunov based sliding mode controller: A finite—Time approach," *Int. J. Control, Autom. Syst.*, pp. 1–11, Dec. 2019.
[3] M.-A. Nasr, S. Nikkhah, G. B. Gharehpetian, E. Nasr-Azadani, and S. H. Hosseinian, "A multi-objective voltage stability constrained energy management system for isolated microgrids," *Int. J. Electr. Power Energy Syst.*, vol. 117, May 2020, Art. no. 105646.
[4] M. Kumar, A. M. Soomro, H. A. Memon, P. Nallagownden, I. Elamvazuthi, and B. Das, "Particle swarm optimization technique based power loss reduction in radial distribution system," *Int. J. Comput. Sci. Netw. Secur.*, vol. 18, no. 12, pp. 88–94, 2018.
[5] M. M. Kumar, A. Alli Rani, and V. Sundaravazhuthi, "A computational algorithm based on biogeography-based optimization method for computing power system security constrains with multi FACTS devices," *Comput. Intell.*, Feb. 2020.
[6] M. Üney and N. Cetinkaya, "New Metaheuristic algorithms for reactive power optimization," *Tehni Ki Vjesnik*, vol. 26, no. 5, pp. 1427–1433, 2019.
[7] J. Wang, S. Chen, and T. T. Lie, "Estimating economic impact of voltage sags," in *Proc. Int. Conf. Power Syst. Technol. (PowerCon)*, vol. 1, Nov. 2004, pp. 350–355.
[8] J. A. Martinez and J. Martin-Arnedo, "Voltage sag analysis using an electromagnetic transients program," in *Proc. IEEE Power Eng. Soc. Winter Meeting. Conf.*, vol. 2, Jan. 2002, pp. 1135–1140.
[9] J. Wang, S. Chen, and T. T. Lie, "A systematic approach for evaluating economic impact of voltage dips," *Electric Power Syst. Res.*, vol. 77, no. 2, pp. 145–154, Feb. 2007.
[10] W. Chen, C. Ding, L. Wang, and X. Zhu, "Economic analysis of voltage sag loss and treatment based on on-site data," in *Proc. China Int. Conf. Electr. Distrib. (CICED)*, Aug. 2016, pp. 1–4.
[11] Z.-L. Gaing, "A particle swarm optimization approach for optimum design of PID controller in AVR system," *IEEE Trans. Energy Convers.*, vol. 19, no. 2, pp. 384–391, Jun. 2004.
[12] S. Chatterjee and V. Mukherjee, "PID controller for automatic voltage regulator using teaching–learning based optimization technique," *Int. J. Electr. Power Energy Syst.*, vol. 77, pp. 418–429, May 2016.
[13] S. Ekinci and B. Hekimoglu, "Improved kidney-inspired algorithm approach for tuning of PID controller in AVR system," *IEEE Access*, vol. 7, pp. 39935–39947, 2019.
[14] M. Rahimian and K. Raahemifar, "Optimal PID controller design for AVR system using particle swarm optimization algorithm," in *Proc. 24th Can. Conf. Electr. Comput. Eng. (CCECE)*, May 2011, pp. 000337–000340.
[15] S. Anbarasi and S. Muralidharan, "Enhancing the transient performances and stability of AVR system with BFOA tuned PID controller," *J. Control Eng. Appl. Inf.*, vol. 18, no. 1, pp. 20–29, 2016.
[16] N. K. Bahgaat and M. A. M. Hassan, "Swarm intelligence PID controller tuning for AVR system," in *Advances in Chaos Theory and Intelligent Control*. Cham, Switzerland: Springer, 2016, pp. 791–804.
[17] M. E. Ortiz-Quisbert, M. A. Duarte-Mermoud, F. Milla, R. Castro-Linares, and G. Lefranc, "Optimal fractional order adaptive controllers for AVR applications," *Electr. Eng.*, vol. 100, no. 1, pp. 267–283, Mar. 2018.
[18] M. Modabbernia, B. Alizadeh, A. Sahab, and M. M. Moghaddam, "Robust control of automatic voltage regulator (AVR) with real structured parametric uncertainties based on $H_\infty$ and $\mu$-analysis," *ISA Trans.*, 2020.
[19] W. Gil-González, O. D. Montoya, and A. Garces, "Standard passivity-based control for multi-hydro-turbine governing systems with surge tank," *Appl. Math. Model.*, vol. 79, pp. 1–17, Mar. 2020.
[20] R. L. A. Ribeiro, C. M. S. Neto, F. B. Costa, T. O. A. Rocha, and R. L. Barreto, "A sliding-mode voltage regulator for salient pole synchronous generator," *Electr. Power Syst. Res.*, vol. 129, pp. 178–184, Dec. 2015.
[21] W. Aribowo, "Focused time delay neural network for tuning automatic voltage regulator," *EMITTER Int. J. Eng. Technol.*, vol. 7, no. 1, pp. 34–43, 2019.
[22] Y. Batmani and H. Golpîra, "Automatic voltage regulator design using a modified adaptive optimal approach," *Int. J. Electr. Power Energy Syst.*, vol. 104, pp. 349–357, Jan. 2019.
[23] G. A. Salman, A. S. Jafar, and A. I. Ismael, "Application of artificial intelligence techniques for LFC and AVR systems using PID controller," *Int. J. Power Electron. Drive Syst.*, vol. 10, no. 3, pp. 1694–1704, 2019.
[24] S. Rakshit and J. Maity, "Three phase, 10 kVA dual conversion type automatic ac voltage regulator–an approach based on fuzzy logic controlled uk converter and PI controlled three phase inverter," in *Proc. IEEE 8th Power India Int. Conf. (PIICON)*, Dec. 2018, pp. 1–6.
[25] M. S. Ayas, "Design of an optimized fractional high-order differential feedback controller for an AVR system," *Electr. Eng.*, vol. 101, no. 4, pp. 1221–1233, Dec. 2019.
[26] L. dos Santos Coelho, "Tuning of PID controller for an automatic regulator voltage system using chaotic optimization approach," *Chaos, Solitons Fractals*, vol. 39, no. 4, pp. 1504–1514, Feb. 2009.
[27] N. Razmjooy, M. Khalilpour, and M. Ramezani, "A new meta-heuristic optimization algorithm inspired by FIFA world cup competitions: Theory and its application in PID designing for AVR system," *J. Control, Autom. Electr. Syst.*, vol. 27, no. 4, pp. 419–440, Aug. 2016.
[28] Z. Bingul and O. Karahan, "A novel performance criterion approach to optimum design of PID controller using cuckoo search algorithm for AVR system," *J. Franklin Inst.*, vol. 355, no. 13, pp. 5534–5559, Sep. 2018.
[29] M. S. Kiran, "TSA: Tree-seed algorithm for continuous optimization," *Expert Syst. Appl.*, vol. 42, no. 19, pp. 6686–6698, Nov. 2015.
[30] I. Gungor, B. G. Emiroglu, A. C. Cinar, and M. S. Kiran, "Integration search strategies in tree seed algorithm for high dimensional function optimization," *Int. J. Mach. Learn. Cybern.*, vol. 11, no. 2, pp. 249–267, Feb. 2020.
[31] W. Chen, M. Cai, X. Tan, and B. Wei, "Parameter identification and State-of-Charge estimation for Li-ion batteries using an improved tree seed algorithm," *IEICE Trans. Inf. Syst.*, vol. E102.D, no. 8, pp. 1489–1497, Aug. 2019.

[32] S. Ekinci, B. Hekimoglu, and E. Eker, "Optimum design of PID controller in AVR system using harris hawks optimization," in *Proc. 3rd Int. Symp. Multidisciplinary Stud. Innov. Technol. (ISMSIT)*, Oct. 2019, pp. 1–6.
[33] H. Gozde and M. C. Taplamacioglu, "Comparative performance analysis of artificial bee colony algorithm for automatic voltage regulator (AVR) system," *J. Franklin Inst.*, vol. 348, no. 8, pp. 1927–1946, Oct. 2011.
[34] M. A. Sahib, "A novel optimal PID plus second order derivative controller for AVR system," *Eng. Sci. Technol., Int. J.*, vol. 18, no. 2, pp. 194–206, Jun. 2015.
[35] A. J. H. Al Gizi, "A particle swarm optimization, fuzzy PID controller with generator automatic voltage regulator," *Soft Comput.*, vol. 23, no. 18, pp. 8839–8853, Sep. 2019.
[36] R. A. Krohling and J. P. Rey, "Design of optimal disturbance rejection PID controllers using genetic algorithms," *IEEE Trans. Evol. Comput.*, vol. 5, no. 1, pp. 78–82, 2001.
[37] T. Kumbasar and H. Hagras, "Big bang–big crunch optimization based interval type-2 fuzzy PID cascade controller design strategy," *Inf. Sci.*, vol. 282, pp. 277–295, Oct. 2014.
[38] N. S. Ozbek and . Eker, "A novel modified delay-based control algorithm with an experimental application," *Inf. Technol. Control*, vol. 48, no. 1, pp. 90–103, 2019.
[39] P. K. Mohanty, B. K. Sahu, and S. Panda, "Tuning and assessment of proportional–integral–derivative controller for an automatic voltage regulator system employing local unimodal sampling algorithm," *Electric Power Compon. Syst.*, vol. 42, no. 9, pp. 959–969, Jul. 2014.
[40] A. A. El-Fergany and H. M. Hasanien, "Tree-seed algorithm for solving optimal power flow problem in large-scale power systems incorporating validations and comparisons," *Appl. Soft Comput.*, vol. 64, pp. 307–316, Mar. 2018.
[41] A. C. Cinar and M. S. Kiran, "A parallel implementation of tree-seed algorithm on CUDA-supported graphical processing unit," *J. Fac. Eng. Archit. Gazi Univ.*, vol. 33, no. 4, pp. 1397–1409, 2018.
[42] B. K. Sahu, S. Panda, P. K. Mohanty, and N. Mishra, "Robust analysis and design of PID controlled AVR system using pattern search algorithm," in *Proc. IEEE Int. Conf. Power Electron., Drives Energy Syst. (PEDES)*, Bengaluru, India, Dec. 2012, pp. 1–6.
[43] U. Güvenç, T. Yi it, A. H. I ik, and . Akkaya, "Performance analysis of biogeography-based optimization for automatic voltage regulator system," *TURKISH J. Electr. Eng. Comput. Sci.*, vol. 24, no. 3, pp. 1150–1162, 2016.

**ERCAN KÖSE** was born in Malatya, Turkey, in 1970. He received the B.S. degree in electrical-electronic engineering from Anadolu University, Eskisehir, Turkey, in 1995, the M.S. degree in electrical-electronic engineering from Eskisehir Osmangazi University, Eskisehir, in 2005, and the Ph.D. degree in electrical-electronic engineering from Sakarya University, Sakarya, Turkey, in 2012.

From 2004 to 2012, he was a Lecturer with Mersin University. From 2012 to 2018, he has been an Assistant Professor with the Mechatronic Engineering Department, Tarsus Technology Faculty, Mersin University. From 2018 to 2019, he has been an Assistant Professor with the Mechatronic Engineering Department, Tarsus University. Since 2020, he has been an Assistant Professor with the Electrical-Electronic Engineering Department, Engineering Faculty, Tarsus University. He is the author of one book chapter, more than 25 articles, and more than 40 conference papers. His research interests include non-linear system control, electric power quality, and intelligent grid systems.